Electronic Density Oscillations in Gold Atomic Chains Assembled Atom by Atom

T. M. Wallis,* N. Nilius, and W. Ho†
Department of Physics and Astronomy and Department of Chemistry, University of California, Irvine, California 92697-4575

(Received 28 July 2002; published 18 November 2002)

Linear Au chains two to 20 atoms long were constructed on a NiAl(110) surface via the manipulation of single atoms with a scanning tunneling microscope. Differential conductance (dI/dV) images of these chains reveal one-dimensional electronic density oscillations at energies 1.0 to 2.5 eV above the Fermi energy. The origin of this delocalized electronic structure is traced to the existence of an electronic resonance measured on single, isolated Au atoms. Variations in the wavelength in dI/dV images of an eleven-atom chain taken at different energies revealed an effective electronic mass of 0.4 ± 0.1 times the mass of a free-electron.

DOI: 10.1103/PhysRevLett.89.236802 PACS numbers: 73.22.–f, 68.37.Ef, 81.07.–b

The scanning tunneling microscope (STM) measures electronic structure at the atomic scale. Specifically, the differential tunneling conductance, dI/dV, is proportional to the local density of electronic states (LDOS) evaluated at the tip apex [1]. This property of the STM underlies scanning tunneling spectroscopy (STS) which has been used to investigate the electronic structure of a wide variety of adsorbates and surfaces with sub-Ångström resolution. STS has been used to investigate the Kondo resonance of single atoms [2,3], the density oscillations of electrons scattered from defects along the length of metallic single walled carbon nanotubes [4], and two-dimensional surface states of metallic substrates [5]. The STM has been used to image one- and two-dimensional electronic standing waves within carbon nanotubes 30 to 40 nm in length [6,7] and surface states within nanoscale metallic islands [8]. In addition, quantum corral experiments employ the capability of the STM to manipulate atoms and molecules to construct nanostructures that act as resonant cavities for two-dimensional surface states of a metallic substrate [9,10].

In this paper, we report the construction of Au atomic chains two to 20 atoms in length on a NiAl surface via the manipulation of single atoms with a STM and the subsequent imaging of one-dimensional electronic density oscillations along their length. The focus of these experiments is upon the electronic features within the nanostructures we have assembled rather than their effect on preexisting surface states. As the atomic chains are of known geometry and are constructed from single atoms, these experiments present an opportunity to probe the relationship between the electronic structure of isolated atoms and the evolution of the electronic structure of metal aggregates as they are constructed atom by atom. The manifestation of quantum mechanical electronic density oscillations in artificially created nanostructures has implications in solid state physics, chemical catalysis and sensors, and nanoscale electronics.

The variable-temperature STM used in these experiments was designed to maximize versatility, stability, and simplicity in operation [11]. All experiments were performed in ultrahigh vacuum (base pressure 3×10^{-11} torr) to prevent contamination of the surface. The STM tips were electrochemically etched from polycrystalline tungsten wire. However, the exact chemical nature of the tip apex is not known because it was deliberately brought into contact with the metal surface before experiments in order to refine the tip apex geometry. Au atoms were thermally evaporated *in situ* from an alumina crucible onto a clean, NiAl(110) crystal at 12 K. Experiments were conducted at this temperature to suppress thermal diffusion of adsorbates.

Single Au atoms adsorbed on the NiAl surface appear as round protrusions in STM images, as shown in Fig. 1. The STS spectrum of an individual Au atom is shown in Fig. 2 and displays a peak in the LDOS 1.95 eV above the Fermi energy with a full-width-half-maximum of 0.40 eV. The measurement of this electronic feature was reproduced for many different atoms and tips with the peak position varying by about 0.10 eV. This electronic resonance is not present in spectra taken with the tip above the bare NiAl surface. The resonance is attributed to the hybridization of Au orbitals with the states of the NiAl substrate. As this resonance is above the Fermi energy, it is not filled in the absence of the tunneling current. No filled electronic resonances were resolved in spectra taken at negative sample bias voltage. The spatial distribution of the electronic resonance was measured by taking a dI/dV image of an individual Au atom, as shown in Fig. 2. The resonance appears as a round feature, 16 Å diam in the dI/dV image.

Single Au atoms were laterally manipulated across the surface following the technique first used for manipulation of individual Xe atoms [12]. In the case of Au atoms on NiAl(110), manipulation of individual atoms was reproducible at tip-sample distances corresponding to a gap resistance of about 0.2 MΩ (e.g., sample bias ~2 mV, tunneling current ~10 nA), though the exact value depended on the configuration of the outermost tip atoms. Observations of the tip height signal during the

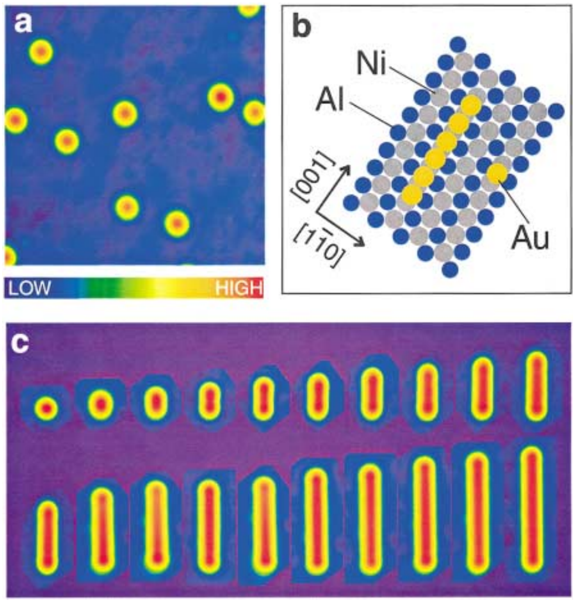

FIG. 1 (color). From single atoms to linear chains of twenty atoms. (a) Individual Au atoms adsorbed on NiAl(110) appear as protrusions in constant current STM topographic images. (b) By lateral manipulation, atoms are brought together to form linear chains along the [001] direction. A schematic shows an individual Au atom and a six-atom chain. (c) STM topographic images from a single Au atom to a linear chain of twenty atoms, arranged in single atom increments from left to right. The images are cut from twenty separate scans, each taken with a sample bias voltage between 2.0 and 2.5 V and a tunneling current between 1.0 and 1.5 nA. Each chain has an apparent height between 2.4 and 2.7 Å. The chains between twelve and twenty atoms long were constructed and imaged with a tip different than the tip used to construct and image the other chains.

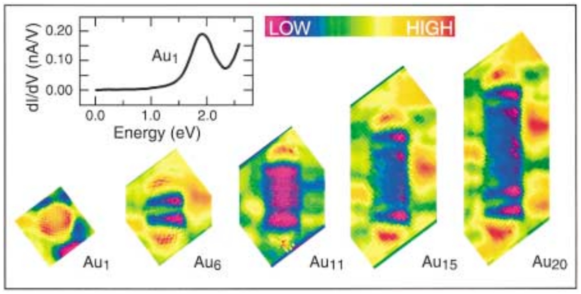

FIG. 2 (color). dI/dV images for a single atom and six-, eleven-, fifteen-, and twenty-atom chains reveal electronic density oscillations. The inset shows a scanning tunneling spectrum taken with the tip positioned directly above a single Au atom showing a peak at 1.95 eV above the Fermi energy. The spectrum was acquired as follows: with the tip positioned directly above a single Au atom and the distance between the tip and the atom fixed, dI/dV was measured using a lock-in technique as a function of the sample bias voltage. The contribution of thermal, instrumental and modulation broadening to the peak width is quite small, about 20 meV. To obtain a dI/dV image, the tip was scanned across the imaging area and dI/dV was measured at regular intervals with the sample bias voltage fixed at a chosen value. A topographic image was acquired simultaneously. The dI/dV image of the atom was taken with a sample bias voltage of 1.95 V. The dI/dV images for the six-, fifteen-, and twenty-atom chains were taken with one tip (tip A) while the dI/dV image for the eleven-atom chain was taken with another tip (tip B). Spectra taken with tip A showed a -0.2 eV shift for all features relative to those in spectra taken with tip B. As a result of this difference, attributed to an electric field effect, the dI/dV image of the eleven-atom chain was acquired with a greater sample bias voltage (2.0 V) than that used to acquire the dI/dV images of the other chains (1.8 V). There were no other prominent tip-dependent effects.

manipulation indicated that the Au atoms were manipulated via a "pulling mode" due to an attractive force between the tip and an atom [13]. The potential barrier for translational motion is small enough to allow for lateral manipulation but sufficiently large that the atom does not hop away during STS scans or dI/dV imaging in which the sample bias voltage reaches a few volts.

By repeated lateral manipulations, individual atoms were brought together to form atomic chains, two to 20 atoms long, shown along with a single Au atom in Fig. 1. The chains were constructed along the [001] direction with each Au atom bridge-bonded to two Ni atoms. Hence, the spacing between atoms in the chain is equal to the spacing between Ni atoms in the [001] direction, 2.89 Å. This distance is quite close to the nearest neighbor separation in bulk Au, 2.88 Å. However, this distance is longer than the Au-Au separation of 2.5 Å in a free dimer [14] and substantially shorter than the nearest neighbor separation of about 3.5 Å measured in stretched Au chains [15,16]. Atoms could be removed from the end of a chain using the same lateral manipulation conditions that were used to add atoms to the end of the chain, indicating that the force needed to remove an atom from the end of a chain was similar to the force required to move an atom from site to site along the surface ($\sim$ 10–100 pN). As the Au atoms are brought within a few Å of one another, their electronic wave functions overlap directly and through the substrate [17]. Because the resonance of the adsorbed Au atoms extends into the substrate, the interaction is delocalized compared to the direct overlap of atomic orbitals in free multimers. Nonetheless, the interaction is sufficiently localized to give rise to distinguishable electronic states along the entire length of the chain, as described below. The suitability of NiAl(110) for the observation of such electronic interactions is attributed to the existence of a pseudogap in the [110] direction for NiAl [18]. In addition, manipulation of metal atoms is feasible on the NiAl(110) surface which provides a quasi-one-dimensional template for chain assembly.

As atoms are added to the chain, the electronic structure increases in complexity due to the interactions among an increasing number of atomic resonances over a broadening range of energies. In addition, the resulting electronic density is expected to vary from point to point along the chain. To explore the spatial distribution of the electronic structure, dI/dV images were taken for the six-, eleven-, fifteen-, and twenty-atom chains at the same energy relative to the lowest electronic feature present in STS spectra taken above the middle of the chain, as shown in Fig. 2. The dI/dV images show a striking pattern of alternating maxima and minima in the electronic density along the length of the chain, even in a chain only six atoms long. The electronic density oscillations bear no obvious relationship to the positions of the atoms within the chains and the constituent atoms could not be resolved in STM topographic images. The electronic structure of the chains is delocalized along their entire length. Even though the Au atomic chains are not isolated from the NiAl substrate, the one-dimensional electronic density oscillations points to predominantly one-dimensional interactions along the chain. The existence of maxima near the ends of the chain has been verified by STS measurements with the tip positioned above the end of the chain. However, the intensity and extent of these maxima is enhanced by edge effects during dI/dV imaging. When the scanning of the tip is paused to make measurements, the position of the tip relative to the sample continues to change due to piezo creep. Because the feedback loop is off during the measurement, a decrease in tip-sample separation will result if the tip is scanning a sharply rising edge of a chain. This decrease in tip-sample separation leads to an enhancement of dI/dV.

In order to better understand the energy dependence of the electronic density oscillations within the atomic chains, dI/dV images were acquired for the eleven-atom chain at sample bias voltages between 1.0 and 2.5 V in 0.1-V increments and are shown in Fig. 3. The number of maxima and minima seen in each dI/dV image increases with increasing sample bias voltage. The emerging peaks and dips in the electronic density oscillations are evident in cross sections of the dI/dV images taken along the chains, as shown in Fig. 4(a). In most of the images, the amplitude and spacing of the extrema within the interior of the chain are nonuniform. However, in the 1.3–1.4, 1.7, and 2.5 V images, we observe more regular patterns with two, three and four minima, respectively. These patterns are reminiscent of the second, third, and fourth excited eigenstates of the familiar one-dimensional particle in a box, though the outermost lobes in the electronic density are enhanced by edge effects during dI/dV imaging.

In the particle-in-a-box model, the distance between consecutive minima in the electronic density is equivalent to one half-wavelength. Thus, a wavelength can be assigned for each state by measuring the average distance between consecutive minima in the relevant cross sections. A parabolic fit to the resulting dispersion relation, shown in Fig. 4(b), yields an effective mass of 0.4 ± 0.1 times the mass of a free electron. The measured wavelengths of the second, third, and fourth excited states correspond to a one-dimensional box 38 ± 2 Å long, in good agreement with the apparent length of the chain in STM topographic images. From this length and the parabolic fit to the dispersion curve, the energies of the ground state and first excited state are predicted to be 0.8 and 1.0 eV, respectively. Assuming that the width of a state within the atomic chain is comparable to the width of the single atom electronic resonance, the ground state and first excited state overlap, as illustrated in Fig. 4(c), and both states contribute to dI/dV images taken with a sample bias voltage near 1.0 V. Similarly, multiple states contribute to dI/dV images taken at intermediate voltages between the second, third, and fourth excited states. The total electronic density seen in dI/dV images taken at voltages where more than one state contributes is a weighted sum of the electronic densities of individual eigenstates. For long chains, such as the sixteen- and twenty-atom chains in Fig. 2, a number of eigenstates are contributing to the electronic density oscillations at all energies between 1.0 and 2.5 eV. For long chains, it is difficult to image pure eigenstates in dI/dV images due to the finite energy width and decreased spacing between the states.

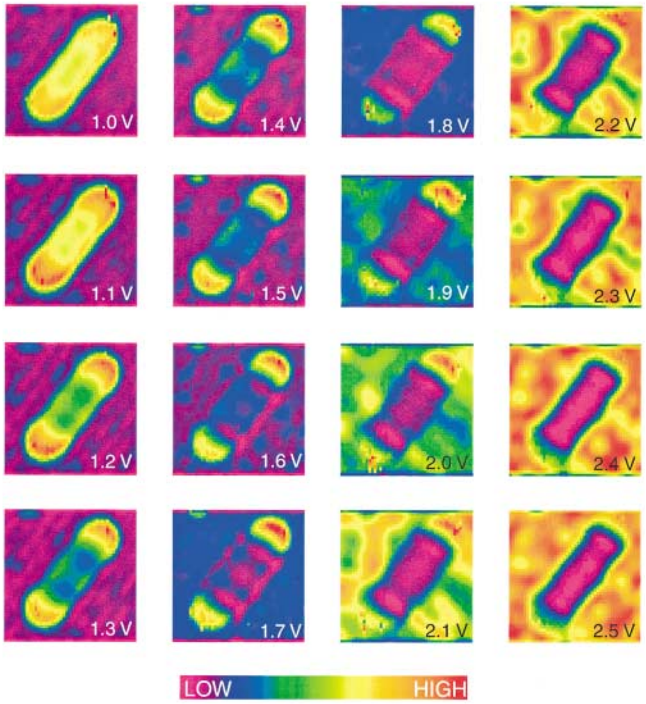

FIG. 3 (color). Sixteen dI/dV images of the eleven-atom chain taken at 0.1 V intervals between 1.0 and 2.5 V. To compensate for the edge effects discussed in the text, each dI/dV image in Figs. 2 and 3 is an average of two scans, one reading dI/dV while the tip is scanned forward and the other while the tip is scanned backward.

This simple particle-in-a-box model of the Au atomic chains does not account for imperfect scattering of the electronic waves at the end of the chains or the coherence length of the broad resonances. The data may also be

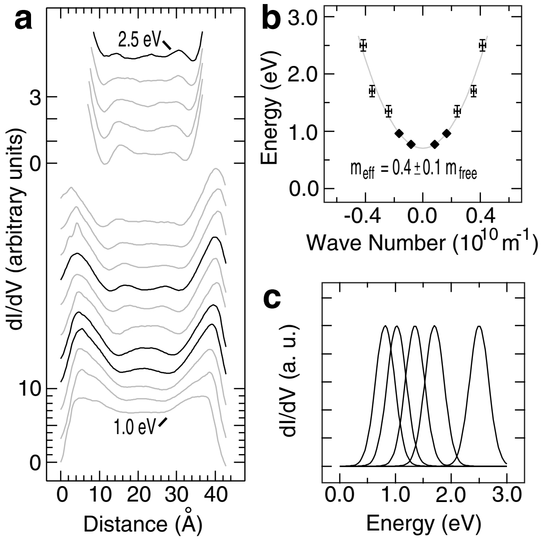

FIG. 4. Electronic density oscillations for eleven-atom chain. Each curve in (a) is an average of five parallel cross sections of one dI/dV image in Fig. 3 taken along the length of the chain. The cross sections are in order of increasing sample bias voltage from bottom to top and have been offset from one another to facilitate comparison. Individual eigenstates dominate the oscillations at 1.3–1.4, 1.7, and 2.5 V (black curves). Wavelengths for these states were measured from the cross sections in (a). For the second excited state, the wavelength was taken to be the average of the wavelengths measured in the 1.3 and 1.4 V cross sections and the energy of the state was taken to be 1.35 eV. The dispersion relation for the eleven-atom chain is shown in (b). A parabolic fit (solid gray line) yields an effective mass of 0.4 times the mass of a free electron. The fit predicts the energies of the ground state and first excited state to be 0.8 and 1.0 eV (solid, black diamonds). In (c), each state is modeled as a normal curve with a full-width-half-maximum equal to that of the resonance of an individual Au atom, 0.40 eV. The second, third, and fourth excited states dominate at 1.35, 1.7, and 2.5 eV. At lower energies, more than one state contribute to the total dI/dV signal.

analyzed with a tight-binding model of the electronic structure of the atomic chains, but in order to distinguish between free-electron and tight-binding behavior, additional data near the edge of the first Brillouin zone is required. A full theoretical description of the system must address the role of the NiAl substrate and, in particular, the role of the pseudogap in the [110] direction for NiAl [18]. A detailed understanding of the dispersion relation and the reduced effective mass may also be obtained from a rigorous theoretical analysis.

In these experiments, we have constructed Au atomic chains by manipulating single atoms with the STM. Electronic density oscillations arising from delocalized, one-dimensional eigenstates of these chains were revealed in dI/dV images. Further studies may examine the evolution of the electronic structure of one- and two-dimensional metal aggregates as they are constructed atom by atom. The potential exists to use the STM to engineer novel metal nanostructures with customized quantum properties and to probe the effects of impurities, alloy formation, and other properties of the solid state at the nanoscale.

This material is based upon work supported by the National Science Foundation under Grant No. 0102887. N. Nilius gratefully acknowledges the Deutsche Forschungsgemeinschaft for support. We are greatly indebted to M. Persson for many stimulating discussions and illuminating calculations. Additional insights have been provided by R. B. Muniz, D. L. Mills, and R. Wu.

---

[*] On leave of absence from Department of Physics, Cornell University, Ithaca, NY 14853-2501.

[†] Corresponding author: wilsonho@uci.edu

[1] J. Tersoff and D. R. Hamann, Phys. Rev. Lett. **50**, 1998 (1983).
[2] J. Li, W.-D. Schneider, R. Berndt, and B. Delley, Phys. Rev. Lett. **80**, 2893 (1998).
[3] V. Madhavan, W. Chen, T. Jamneala, M. F. Crommie, and N. S. Wingreen, Science **280**, 567 (1998).
[4] M. Ouyang, J.-L. Huang, and C. M Lieber, Phys. Rev. Lett. **88**, 066804 (2002).
[5] Y. Hasegawa and Ph. Avouris, Phys. Rev. Lett. **71**, 1071 (1993).
[6] L. C. Venema, J. W. G. Wildoer, J. W. Janssen, S. J. Tans, H. L. J. T. Tuninstra, L. P. Kouwenhoven, and C. Dekker, Science **283**, 52 (1999).
[7] S. G. Lemay, J. W. Janssen, M. van den Hout, M. Mooij, M. J. Bronikowski, P. A. Willis, R. E. Smalley, L. P. Kouwenhoven, and C. Dekker, Nature (London) **412**, 617 (2001).
[8] J. Li, W.-D. Schneider, R. Berndt, and S. Crampin, Phys. Rev. Lett. **80**, 3332 (1998).
[9] M. F. Crommie, C. P. Lutz, and D. M. Eigler, Nature (London) **363**, 524 (1993).
[10] E. J. Heller, M. F. Crommie, C. P. Lutz, and D. M. Eigler, Nature (London) **369**, 464 (1994).
[11] B. C. Stipe, M. A. Rezaei, and W. Ho, Rev. Sci. Instrum. **70**, 137 (1999).
[12] D. M. Eigler and E. K. Schweizer, Nature (London) **344**, 524 (1990).
[13] L. Bartels, G. Meyer, and K.-H. Rieder, Phys. Rev. Lett. **79**, 697 (1997).
[14] H. Häkinnen, R. N. Barrett, and U. Landman, J. Phys. Chem. B **103**, 8814 (1999).
[15] A. I. Yanson, G. R. Bollinger, H. E. van den Brom, N. Agrait, and J. M. van Ruitenbeek, Nature (London) **395**, 783 (1998).
[16] H. Ohnishi, Y. Kondo, and K. Takayanagi, Nature (London) **395**, 780 (1998).
[17] N. Nilius, T. M. Wallis, W. Ho, and M. Persson (unpublished results).
[18] S.-C. Lui, M. H. Kang, E. J. Mele, E. W. Plummer, and D. M. Zehner, Phys. Rev. B **39**, 13149 (1989).